$\bar{p}p \to \bar{\Xi}\Xi$ reaction in the meson exchange picture

J. Haidenbauer*
Department of Physics and Mathematical Physics, University of Adelaide, Adelaide 5001, Australia

K. Holinde and J. Speth
Institut für Kernphysik, Forschungszentrum Jülich GmbH, W-5170 Jülich, Germany
(Received 29 December 1992)

The strangeness production process $\bar{p}p \to \bar{\Xi}\Xi$ is investigated in a meson exchange model and a full coupled channel treatment. Results for cross sections, polarizations, and singlet fractions are presented and compared with those obtained from quark-gluon models. Characteristic differences occur in the $(\bar{p}p \to \bar{\Xi}^-\Xi^-)/(\bar{p}p \to \bar{\Xi}^0\Xi^0)$ cross section ratios.

PACS number(s): 25.43.+t, 13.75.Cs, 21.30.+y

The proposed SuperLEAR facility at CERN promises access to a great variety of new physics [1]. One particular class of reactions that could be studied are processes of the kind $\bar{p}p \to \bar{H}H$, where H can be any strange or charmed hadron [2]. An interesting case is the production of a $\bar{\Xi}\Xi$ pair which has its threshold at around 2.62 GeV/c, i.e., at the lower-energy range covered by the SuperLEAR proposal.

The Ξ particles [$\Xi^0(1314.5)$, $\Xi^-(1321.32)$] are located at the lower corners of the SU(3) $J=\frac{1}{2}^+$ baryon octet and therefore a change in strangeness of $\Delta S=2$ is required in their production in $\bar{N}N$ collisions. In the constituent quark model this means that two of the quarks in each initial hadron have to annihilate, cf. Fig. 1, whereas in the meson-exchange picture two mesons carrying strangeness have to be exchanged (Fig. 2). Such processes can take place only at rather short distances and it is therefore believed that the $\bar{p}p \to \bar{\Xi}\Xi$ reaction is a much better place for establishing the relevance of quark-gluon degrees of freedom in the strangeness production process than $\bar{p}p \to \bar{\Lambda}\Lambda$ or $\bar{p}p \to \bar{\Lambda}\Sigma^0, \bar{\Sigma}^0\Lambda$, say, which require only a change in strangeness by one unit. Furthermore, the $\bar{p}p \to \bar{\Xi}\Xi$ process could be also very useful for testing fundamental symmetries such as CP violation in hyperon decay [1].

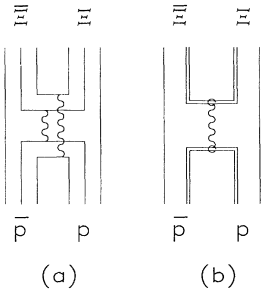

FIG. 1. The $\bar{p}p \to \bar{\Xi}\Xi$ transition in the constituent-quark model. (a) Double annihilation of quarks as considered in Ref. [5]. (b) Annihilation of a diquark as studied by Kroll and coworkers [3,4].

The lack of accurate data together with the (aforementioned) more complicated transition mechanism has so far curtailed the $\bar{p}p \to \bar{\Xi}\Xi$ process from having wider attention from the theorists. In fact, we are aware of only two pertinent calculations, both based on quark-gluon dynamics [3–5]. Therefore, in this work, we want to present results of a first exploratory investigation of the $\bar{p}p \to \bar{\Xi}\Xi$ transition in the framework of conventional meson exchange. It is an extension of our recently published coupled channel model for antihyperon-hyperon production, where $\bar{p}p \to \bar{\Lambda}\Lambda$, $\bar{p}p \to \bar{\Lambda}\Sigma^0, \bar{\Sigma}^0\Lambda$, as well as $\bar{p}p \to \bar{\Sigma}\Sigma$ transitions have been considered [6,7].

In the meson-exchange picture the interactions of baryons and antibaryons are related via G parity and/or charge conjugation. Such relations have been used extensively in Refs. [6,7] to constrain the interaction forces in and between the various considered channels $(\bar{N}N, \bar{\Lambda}\Lambda, \bar{\Lambda}\Sigma, \bar{\Sigma}\Lambda, \bar{\Sigma}\Sigma)$ as much as possible. To be more specific, the elastic part of the $\bar{N}N$ interaction has been obtained from an energy-independent one-boson-exchange (OBE) version (OBEPF of Ref. [8]) of the Bonn NN potential [9], while the (elastic part of the) diagonal $\bar{Y}Y$ interactions as well as $\bar{Y}Y \to \bar{Y}Y$ and $\bar{N}N \to \bar{Y}Y$ transitions have been derived from the hyperon-nucleon model A of Ref. [10]. Thereby, in general, coupling constants but also form factors at the baryon-baryon-meson vertices have been kept exactly the same as in the NN and

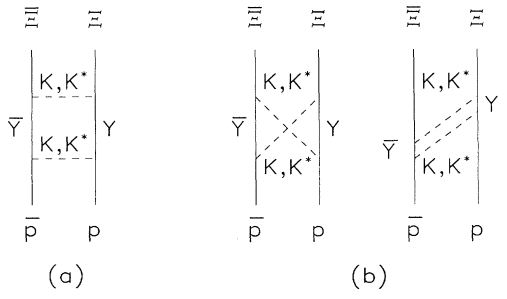

FIG. 2. The $\bar{p}p \to \bar{\Xi}\Xi$ transition in the meson exchange picture. Y stands for Λ and Σ. (a) Iterative box diagrams included in our model calculation. (b) Some noniterative contributions.

*Present address: Institut für Theoretische Physik, Universität Graz, A-8010 Graz, Austria.

hyperon-nucleon sector. The annihilation part of both the $\bar{N}N$ and (diagonal) $\bar{Y}Y$ interactions has been parametrized by means of a spin-dependent, isospin- and energy-independent optical potential. For $\bar{N}N$ the strength parameters and range have been determined independently by a fit to the empirical $\bar{p}p \to \bar{p}p$ and $\bar{p}p \to \bar{n}n$ cross sections in the relevant energy range. The corresponding parameters occurring in the annihilation part of the various $\bar{Y}Y$ interactions have been determined by a fit to the existing $\bar{p}p \to \bar{\Lambda}\Lambda$, $\bar{p}p \to \bar{\Lambda}\Sigma^0, \bar{\Sigma}^0\Lambda$, and $\bar{p}p \to \bar{\Sigma}^+\Sigma^+$ cross sections [6,7].

For the extension to the $\bar{\Xi}\Xi$ channel the situation is somewhat different. Firstly the now-required additional vertices do not occur in our hyperon-nucleon model [10] because the Ξ does not couple directly to the nucleon. Still the coupling constants at the various Ξ vertices follow from the same SU(3) relations, which have been used already in Ref. [10] to determine the hyperon-nucleon coupling strengths. [An exception constitutes the $\Xi\Xi\sigma$ coupling, since in the Bonn-Jülich hyperon-nucleon model the σ stands for the correlated $\pi\pi$ s-wave interaction and is neither considered to be an SU(3) singlet nor a member of the 0^+-meson octet. The value for the coupling constant used in our calculations is roughly the same as for the $\Sigma\Sigma\sigma$ coupling.] However, we have no information about the corresponding cutoff masses. Secondly, no reliable experiments are available, which would allow us to constrain the free parameters of the annihilation part of the $\bar{\Xi}\Xi$ interaction.

As far as the cutoff masses are concerned we decided to take values from corresponding nucleon-hyperon-meson and hyperon-hyperon-meson vertices. Such a choice actually suggests itself, since in most cases those cutoff masses at particular meson vertices are very similar or even identical (cf. Table 3a of Ref. [10]). Moreover, test calculations showed that the results are not too sensitive to moderate variations of those cutoff masses. For example, using a cutoff of 1.2 GeV instead of 2.0 GeV at the $\Xi\Lambda K$ vertex resulted only in a 5% change of the total $\bar{p}p \to \bar{\Xi}\Xi$ cross sections. The parameters used at the various Ξ vertices are listed in Table I.

The choice of the $\bar{\Xi}\Xi$ annihilation part is certainly more crucial. Here we adopt the parameters found for the $\bar{\Sigma}\Sigma$ channel in Ref. [7]. Employing the parameter sets of the $\bar{\Lambda}\Lambda$ or $\bar{\Lambda}\Sigma, \bar{\Sigma}\Lambda$ annihilation parts would lead, in fact, to an enhancement of the $\bar{p}p \to \bar{\Xi}\Xi$ cross sections of up to 50%. Since in those cases most of the additional contributions come, however, from a peak at the very backward region, where we expect the differential cross section to be rather smooth, as is the case for $\bar{p}p \to \bar{\Lambda}\Lambda$ and $\bar{p}p \to \bar{\Lambda}\Sigma^0, \bar{\Sigma}^0\Lambda$ [6,7], we consider those particular choices for the $\bar{\Xi}\Xi$ annihilation part as not very realistic.

TABLE I. Coupling constants and cutoff masses at the Ξ vertices. The coupling constants are obtained from SU(3) relations with $g_{NN\pi}/\sqrt{4\pi}=3.795$, $g_{NN\rho}/\sqrt{4\pi}=0.917$, and $f_{NN\rho}/\sqrt{4\pi}=5.591$ and the $F/(F+D)$ ratios $\alpha_{ps}=2/5$, $\alpha_v^e=1$, and $\alpha_v^m=2/5$.

Vertex	$g_\alpha/\sqrt{4\pi}$	$f_\alpha/\sqrt{4\pi}$	Λ_α (GeV)
$\Xi\Lambda K$	1.315		2.0
$\Xi\Sigma K$	−3.795		2.0
$\Xi\Lambda K^*$	1.588	0.666	2.2
$\Xi\Sigma K^*$	−0.917	−5.591	2.2
$\Xi\Xi\pi$	−0.759		1.3
$\Xi\Xi\rho$	0.917	−2.219	1.3
$\Xi\Xi\omega$	1.491	−2.800	2.0
$\Xi\Xi\sigma$	3.162		1.7

The basic transition mechanism for $\bar{p}p \to \bar{\Xi}\Xi$, generated by our coupled channel model, is depicted in Fig. 2(a). As in our former $\bar{p}p \to \bar{Y}Y$ studies [6,7] we did not take into account other (noniterative) two-meson exchange diagrams such as those shown in Fig. 2(b) in this exploratory investigation. The importance of such processes remains to be investigated. The present calculation is done in the isospin basis. The reproduction of the empirical thresholds for $\bar{p}p \to \bar{\Xi}^0\Xi^0$ as well as $\bar{p}p \to \bar{\Xi}^-\Xi^-$ is ensured by using either the Ξ^0 or the Ξ^- mass in the corresponding calculations.

Results for the total cross sections are shown in Fig. 3. Note that the experimental values represent only upper bounds for the cross sections, deduced from an experiment where actually no $\bar{p}p \to \bar{\Xi}^0\Xi^0$ or $\bar{p}p \to \bar{\Xi}^-\Xi^-$ events were detected [11]. Differential cross sections and polarizations at $p_{\rm lab}=2.7$ GeV/c are depicted in Figs. 4 and 5. For $\bar{p}p \to \bar{\Xi}^0\Xi^0$ we observe a marked forward peak of the differential cross section as it is known also from other $\bar{p}p \to \bar{Y}Y$ reactions [6,7]. The result for $\bar{p}p \to \bar{\Xi}^-\Xi^-$ on the other hand is relatively flat. It is similar to the one for the $\bar{p}p \to \bar{\Sigma}^-\Sigma^-$ transition [7] which, like $\bar{p}p \to \bar{\Xi}\Xi$, can occur only in a two-step process. It is interesting that also the quark-gluon transition model of Kroll, Quadder, and Schweiger predicts rather flat differential cross sections for such two-step processes [4].

The singlet fraction $F_s=\frac{1}{4}(1-\langle \sigma_{\bar{Y}}\cdot\sigma_Y\rangle)$ has been very useful in studying the characteristics of $\bar{p}p \to \bar{Y}Y$ reactions. For example, it has been found that the $\bar{p}p \to \bar{\Lambda}\Lambda$ reaction takes place primarily in triplet states [12,6]. The same seems to be true also for $\bar{p}p \to \bar{\Sigma}\Sigma$ [7]. The $\bar{p}p \to \bar{\Lambda}\Sigma^0, \bar{\Sigma}^0\Lambda$ process, on the other hand, involves significant contributions also from singlet states [7]. For $\bar{p}p \to \bar{\Xi}^-\Xi^-(\bar{\Xi}^0\Xi^0)$ the angle-averaged value for F_s (at 2.7

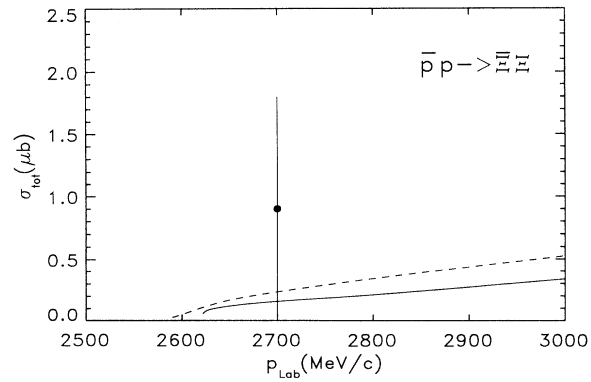

FIG. 3. Total $\bar{p}p \to \bar{\Xi}^-\Xi^-$ (solid line) and $\bar{p}p \to \bar{\Xi}^0\Xi^0$ (dashed line) cross sections as predicted by our coupled-channel model. The experiment is an upper bound for $\bar{p}p \to \bar{\Xi}^-\Xi^-$ taken from Ref. [11].

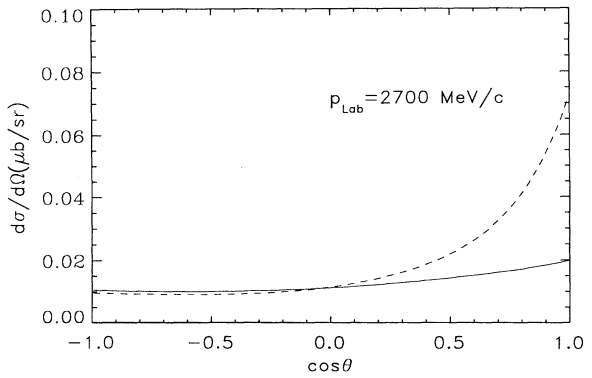

FIG. 4. Differential cross sections for the $\bar{p}p \to \bar{\Xi}\Xi$ processes at $p_{\rm lab} = 2.7$ GeV/c. Same description of the curves as in Fig. 3.

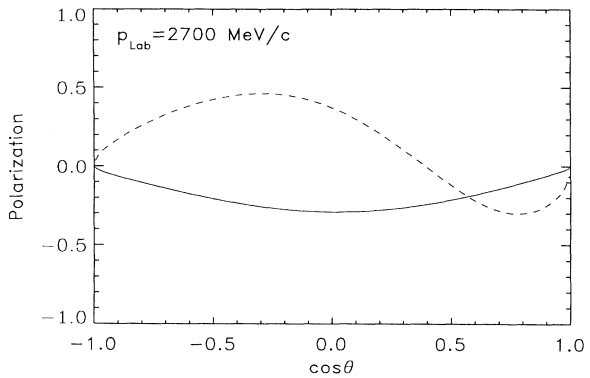

FIG. 5. Ξ polarization for the $\bar{p}p \to \bar{\Xi}\Xi$ processes at $p_{\rm lab} = 2.7$ GeV/c. Same description of the curves as in Fig. 3.

GeV/c) turns out to be 0.38 (0.20), which roughly corresponds to an equal population of spin singlet and spin triplet final states, similar to $\bar{p}p \to \bar{\Lambda}\Sigma^0, \bar{\Sigma}^0\Lambda$. A difference occurs, however, in the angular dependence: In the latter reaction the singlet fraction is nearly independent of the scattering angle; now it is almost zero in forward direction, i.e., the $\bar{\Xi}\Xi$ pair is produced predominantly in triplet states, whereas the backward region is dominated by singlet transitions.

Since in our model the $\bar{p}p \to \bar{\Xi}\Xi$ reaction can proceed via $\bar{\Lambda}\Lambda$, $\bar{\Lambda}\Sigma$, $\bar{\Sigma}\Lambda$ as well as $\bar{\Sigma}\Sigma$ intermediate states the question arises whether any of those transition channels is dominant. Therefore we carried out further calculations where we switched off all but one of the $\bar{Y}Y \to \bar{\Xi}\Xi$ transitions. We found that all transitions are of comparable magnitude with $\bar{p}p \to \bar{\Lambda}\Lambda \to \bar{\Xi}\Xi$ being the largest one. Furthermore, we noticed that there are considerable cancellations between the contribution from the various $\bar{p}p \to \bar{Y}Y \to \bar{\Xi}\Xi$ transitions. These cancellations affect mostly the triplet states, which explains why the singlet fraction for $\bar{p}p \to \bar{\Xi}\Xi$ is relatively large.

Let us now compare our results with two model calculations based on quark-gluon dynamics. The work of Genz and collaborators [5] is based on the transition mechanism shown in Fig. 1(a), i.e., the double annihilation of quarks. The annihilation is parametrized either by an intermediate gluon (gl) or [vector (v) or pseudovector (ps)] meson states. The model of Kroll and coworkers [3,4] builds on the assumption that two of the three quarks in the hadrons form a quasibound state, a so-called diquark, which then acts as an elementary particle. The $\bar{\Xi}\Xi$ pair is then produced by the annihilation of such a diquark via an intermediate gluon [cf. Fig. 1(b)]. Cross-section predictions obtained by these authors are listed in Table II together with our values and some experiments [11,13].

The results from the meson-exchange model are, in general, substantially smaller compared to those derived from the constituent quark model (with the exception of the ps model of Ref. [5]). However, we do not believe that this difference is necessarily inherent to the different transition dynamics. The reason is that in the quark-model calculations initial- and final-state interactions have been neglected. In particular, the latter should be very important for the beam momenta considered here (since the kinetic energy in the $\bar{\Xi}\Xi$ system is small) and may reduce the quark model results by even an order of magnitude, as demonstrated by Kohno and Weise for $\bar{p}p \to \bar{\Lambda}\Lambda$ [14].

There are further remarkable differences: The $\bar{p}p \to \bar{\Xi}^0\Xi^0$ and $\bar{p}p \to \bar{\Xi}^-\Xi^-$ cross sections obtained with our meson exchange model are of comparable size with the latter being somewhat smaller, a result that proved to be rather stable against the choice of parameters. In the

TABLE II. Total cross sections (in μb) for the $\bar{p}p \to \bar{\Xi}^0\Xi^0$ and $\bar{p}p \to \bar{\Xi}^-\Xi^-$ reactions.

$p_{\rm lab}$ (GeV/c)	Present work	Kroll, Quadder, and Schweiger [4]	Genz, Nowakowski, and Woitschitzky [5] gl	v	ps	Expt.
			$\bar{p}p \to \bar{\Xi}^-\Xi^-$			
2.7	0.16	2.61				≤ 1.8[a]
3.0	0.34	4.95	7.4	1.9	0.01	2 ± 1[b]
3.5	0.76	6.02	8.6	2.3	0.01	≤ 1[b]
			$\bar{p}p \to \bar{\Xi}^0\Xi^0$			
2.7	0.23	0.95				≤ 2.8[a]
3.0	0.53	1.65	3.8	1.0	0.05	
3.5	1.03	1.84	4.4	1.2	0.06	

[a]Reference [11].
[b]Reference [13].

constituent quark model, on the other hand, the $\bar{p}p \to \bar{\Xi}^- \Xi^-$ cross sections are predicted to be larger—in fact, even by a factor 2 to 3. As a consequence some quark model predictions for $\bar{p}p \to \bar{\Xi}^- \Xi^-$ considerably overshoot the sparse experimental evidence (cf. Table II). In those transition models derived from quark-gluon dynamics the ratio of $\bar{\Xi}^- \Xi^-$ to $\bar{\Xi}^0 \Xi^0$ production is essentially determined by the overlap of the SU(6) spin-flavor wave functions. Therefore, the difference in this ratio may indeed by characteristic for the specific transition scenario.

Table II also shows that the production cross sections are very sensitive to the quantum numbers attributed to the (quark) annihilation vertex. The results for an intermediate pseudoscalar meson are, e.g., about 2 orders of magnitude smaller than the others.

Finally we want to point out that at the present state our meson-exchange approach and the two models based on quark-gluon dynamics, respectively, have rather complementary character. In the latter it is assumed that the $\bar{\Xi}\Xi$ pair production is governed by direct transitions as shown in Fig. 1. Other possible transition mechanisms such as, e.g., consecutive single-quark annihilation with intermediate ($\bar{\Lambda}\Lambda$, etc.) states are completely neglected (as are all effects from initial- and final-state distortions). Such two-step processes provide, however, the basic transition mechanism in our meson-exchange model. On the other hand, as mentioned above, we did not take into account possible noniterative two-meson exchange transitions such as those shown in Fig. 2(b). Indeed these processes may roughly correspond to the direct transitions considered in the constituent quark model.

We thank Dr. N. Hamann for initiating this work. Furthermore, we would like to thank Dr. W. Schweiger for several clarifying comments and for communicating the results of his calculations to us. This work was supported by the Australian Research Council and the NATO Grant No. Rg 85/0093.

[1] C. B. Dover, *Proceedings of the SUPERLEAR Workshop, Zürich, 1991,* Institute of Physics Conference Series No. 124, p. 421.

[2] W. Oelert, in *Proceedings of the SUPERLEAR Workshop, Zürich, 1991* (Ref. [1]), p. 307.

[3] P. Kroll and W. Schweiger, Nucl. Phys. **A474**, 608 (1987).

[4] P. Kroll, B. Quadder, and W. Schweiger, Nucl. Phys. **B316**, 373 (1989).

[5] H. Genz, M. Nowakowski, and D. Woitschitzky, Phys. Lett. B **260**, 179 (1991).

[6] J. Haidenbauer, T. Hippchen, K. Holinde, B. Holzenkamp, V. Mull, and J. Speth, Phys. Rev. C **45**, 931 (1992); J. Haidenbauer, K. Holinde, V. Mull, and J. Speth, *ibid.* **46**, 2158 (1992).

[7] J. Haidenbauer, K. Holinde, and J. Speth, Phys. Rev. C **46**, 2516 (1992).

[8] J. Haidenbauer, K. Holinde, and M. B. Johnson, Phys. Rev. C **45**, 2055 (1992).

[9] R. Machleidt, K. Holinde, and Ch. Elster, Phys. Rep. **149**, 1 (1987).

[10] B. Holzenkamp, K. Holinde, and J. Speth, Nucl. Phys. **A500**, 485 (1989)

[11] G. P. Fisher *et al.*, Phys. Rev. **161**, 1335 (1967).

[12] R. G. E. Timmermans, Th. A. Rijken, and J. J. de Swart, Phys. Lett. **275B**, 227 (1991).

[13] B. Musgrave *et al.*, Nuovo Cimento **35**, 735 (1965).

[14] M. Kohno and W. Weise, Nucl. Phys. **A479**, 433c (1988).